



# WIDELY TUNABLE FILTER TECHNOLOGY & MEASUREMENT OF CRITICAL SPECIFICATIONS

BY DANIEL GAGNON AND LAURA-ISABELLE DION-BERTRAND

## 1\_ ABSTRACT

The out-of-band rejection and the optical density (OD) are two critical specifications of tunable filters. Unfortunately these properties are often misinterpreted and their definitions tend to differ from one manufacturer to another. End users need to be careful when looking over the specifications of a filter. Also, the measurement of these properties for customers can be laborious. One needs to have sensitive instruments with a high dynamic range, a wide spectral range and a high power source. In this white paper, clear and rigorous definitions of the out-of-band rejection and the OD of widely tunable filters are presented, and the steps and instrumentation needed to accurately measure those specifications are exposed.

## 2\_ THE CHALLENGE

Due to the broad variety of technologies and companies offering similar products, choosing the best tunable filter for a given experiment can be difficult. It gets even harder when the definition of certain requirements vary from one manufacturer to another. Since each filter possesses its own strengths and weaknesses, comparing their equivocal specifications can become a puzzling challenge. The aim of this white paper is to rigorously define the most relevant specifications of widely tunable filters, emphasizing on the Laser Line Tunable Filter (LLTF) Contrast™, and more generally, to inform customers on how to measure these critical specifications.

The unique ability of the aforementioned filter to strongly isolate a narrow band of light will become clear once the notions of optical density and out-of-band rejection (sometimes referred to as "isolation" or even "optical density") are accurately defined and understood. The correct evaluation of these specifications is challenging since only high sensitivity and ultra-low noise measurement setups can provide precise and reliable results. Before tackling this challenge of measuring the specifications, we will start by defining terminology standards. This common base will allow us to adequately compare different technologies.

### 3\_ ESTABLISHING TERMINOLOGY

The notion of band rejection is mainly used in signal processing to define the ability of a filter to separate the wanted signal from the unwanted one, on a specific frequency band. Bandpass and stopband filters are all rejection filters following this definition; the first allows a specific frequency to be transmitted and blocks the rest, while the second blocks a specific frequency and lets the rest go through. This concept can be applied to the field of optics to define **the ability of an optical bandpass filter to select precise wavelengths, but to attenuate to very low levels those outside a specific band.** Sometimes incorrectly referred to as "isolation" or "optical density", the out-of-band rejection is the appropriate term, which we will use here, to specify this property. Out-of-band rejection is defined relatively to the peak efficiency of a filter: it defines a rejection value, commonly in dB, outside a given wavelength band centered around  $\lambda_c$ . FIG. 1 illustrates this concept. As an example, a band of  $\pm 45$  nm is presented and, outside this band, a rejection level (for unwanted wavelengths) of -60 dB is obtained. For instance, on a specification sheet, one would find the corresponding property: out-of-band rejection  $< -60$  dB @  $\lambda_c \pm 45$  nm.

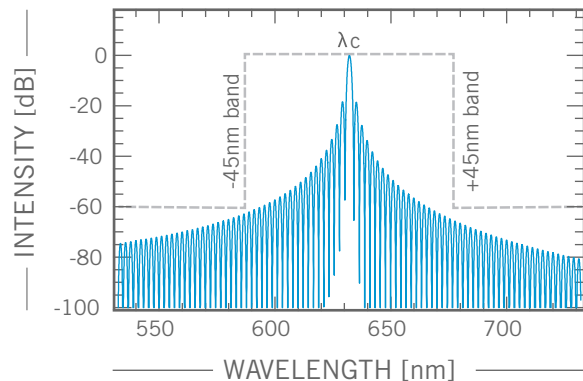


FIG. 1 : Illustration of the out-of-band rejection of a volume holographic grating at  $\lambda_c = 632$  nm. Bands of  $\pm 45$  nm are presented and an out-of-band rejection of -60 dB is obtained.

In the case of the LLTF Contrast™ we define 2 sets of bands. The first is  $\lambda_c \pm 40$  nm for the visible (VIS) version of the instrument (400-1000 nm), and the second  $\lambda_c \pm 80$  nm for the short wavelength infrared (SWIR) version (1000-2300 nm). The biggest challenge regarding this specification is to measure it. The limitations usually come from the dynamic range and the noise limit of the measurement setup. To overcome these, one needs very sensitive instruments with a high dynamic range, coupled to a relatively high power broadband source or tunable laser.

Another characteristic of importance, the optical density (OD), is often confused with the out-of-band rejection. In spectroscopy, the optical density (also referred to as absorbance in material science) of an instrument **is the logarithmic ratio between the radiated power of the incident beam and the radiated power transmitted through the instrument.** Using the transmittance definition, the OD can be expressed as:

$$\begin{aligned} \text{OD} &= \log_{10}(I_0/I_t) \\ &= \log_{10}(T^{-1}) \\ &= -\log_{10}(T) \end{aligned}$$

where T is the transmittance ( $T=I_t/I_0$ ),  $I_t$  the transmitted light intensity and  $I_0$  the incident light intensity. Optical density is a way to describe the ability of an optical filter to block unwanted wavelengths.

1. dB (decibel) is a logarithmic unit corresponding to one tenth of one bel, and is used to express the ratio between two values. In the case of a power ratio, it is equal to ten times the base 10 logarithm of the ratio of two power quantities :  $\text{dB}=10\log_{10}(P_1/P_0)$ .

2. The dynamic range is the ratio between the largest and smallest measurable quantity of instrument.

The next sections explain in more details the particular properties of the LLTF Contrast™ as well as the experimental setup needed for the measurement of the out-of-band rejection and OD.

### 3.1\_ THE MAIN ASSETS OF THE LLTF CONTRAST™

Now that the notions of out-of-band rejection and optical density are well defined, one can fully understand the potential of the LLTF Contrast™ (FIG. 2). It is a non-dispersive, sub-nanometric bandpass optical filter. It has a high efficiency (up to 65 % including all polarisations and coupling losses) possesses a high out-of-band rejection ( $< -60$  dB), and high optical density ( $> OD 6.5$ ). The aforementioned efficiency refers to the signal throughput, defined as the ratio of the filtered intensity over the input intensity at a specific wavelength. The LLTF Contrast™ is also a widely tunable optical filter. Based on volume Bragg gratings (VBG), a specific configuration will allow this resonant filter to select a narrow portion of a laser spectrum (monochromatic or broadband). Additional information on the fundamentals of volume holographic gratings can be found in Appendix 1. In comparison to other commercially available filters, it provides a wide tunability: from 400 to 1000 nm for the VIS option and from 1000 to 2300 nm for the SWIR range, with bandwidths below 2.5 nm and 5 nm respectively. The bandwidth refers to the spectral Full Width at Half Maximum (FWHM) of the filtered beam also at a specific wavelength (see Appendix 2, FIG. A2). A major benefit of this technology is its superior out-of-band rejection ( $< -60$  dB) [1]. This instrument is the only tunable optical filter with an optical density higher than OD 4. In order to establish those specifications, accurate performance and quality control tests had to be performed on highly sensitive setups which are describe in section 4.

One of the main use of this instrument is the production of an ultrabroadband tunable laser source. This unique source is obtained by the combination of the tunable filter and a commercial supercontinuum source. More information on the properties of the ultrabroad tunable laser source can be found in Appendix 2.



FIG. 2 : Photon etc's Laser Line Tunable Filter (LLTF) Contrast™ .

## 4\_ HOW TO MEASURE THE OUT-OF-BAND REJECTION AND OD

As previously stated, the ideal instruments to measure the out-of-band rejection and OD should have a high dynamic range and a high sensitivity. A sufficient spectral resolution [2] is also required, ideally lower than one fourth of the FWHM to avoid sampling and convolution, to spectrally resolve the diffraction efficiency of the tunable filter. Such an ideal setup can be assembled out of commercially available instrumentation, but a few adaptations should be made to obtain precise and accurate measurements. Of course, the optical specifications of the filter and the laser source need to be taken into account. The requirements concerning the measuring instruments are as follow:

Dynamic Range > 70 dB  
Sensitivity < -80 dBm<sup>3</sup>  
Wavelength span > out-of-band limits

The dynamic range must be higher than the specified out-of-band rejection (< -60 dB) and optical density (> OD 6.5). Indeed, an insufficient dynamic range will result in saturated measurements if the detector is too sensitive, or in noise limited measurements if the filter is coupled to a high power sources. Furthermore, the sensitivity must be as high as possible to reduce the measurement's noise floor. Since the power density involved is low (a few mW/nm), it is important to be able to measure weak power. Ideally, the instrument should measure power down to a few pW to reach the noise floor of the filter and avoid an insufficient detection limit of the measuring instrument itself. Finally, the spectral range should cover, at least, a window including the out-of-band wavelength limits ( $\lambda_c \pm X$  nm) in order to see the full spectral shape of the VBG. Measurements outside of these out-of-band limits should also be performed to validate the rejection span.

Following these requirements, Charge Coupled Devices (CCD) or Complementary Metal Oxide Semiconductor (CMOS) cameras coupled to a spectrometer are fairly good candidates, but would be pushed to their limits. Another strategy consists in coupling a monochromator to a low noise amplification chain photodiode. This setup will allow power measurements in a range covering 20 dBm to -85 dBm with off-the-shelf commercial devices. For these reasons, the best solution consists in using an Optical Spectrum Analyser (OSA): it possesses the right wavelength span and sensitivity.

A realistic representation of the measurement setup used by Photon etc. to obtain the out-of-band rejection and the OD is depicted in FIG. 3, where the external source is a supercontinuum (SC) laser. Throughout the manufacturing and qualification processes, the equivalent of two light paths are created within the LLTF: one passing through the VBG to collect the filtered light, while another passes through the mirrors, M1-4 (dotted line), where all the power from the SC is collected.

---

3. dBm has de same definition than a decibel, except that the power ratio is relative to 1 mW :  $10\log_{10}(P_1/1 \text{ mW})$ .

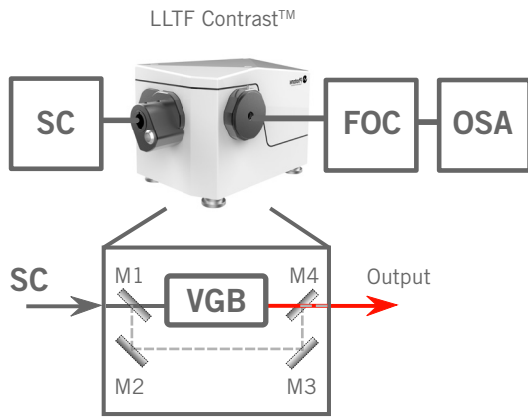


FIG. 3 : Realistic representation of the measurement setup used to measure the out-of-band rejection and the optical density. SC : Fianium’s supercontinuum source SC-400-4, FOC : Fiberoptic Output Coupler (using achromatic 10 mm focal lens, multimode 50/62.5  $\mu\text{m}$ ), OSA : Optical Spectrum Analyser ANDO AQ6315E, M1-4: mirrors, VBG : Volume Bragg Grating. two light paths are created within the LLTF: one goes through the VBG to collect the filtered light, while another through mirrors, M1-4 (dotted line), and where all the power from the SC is collected.

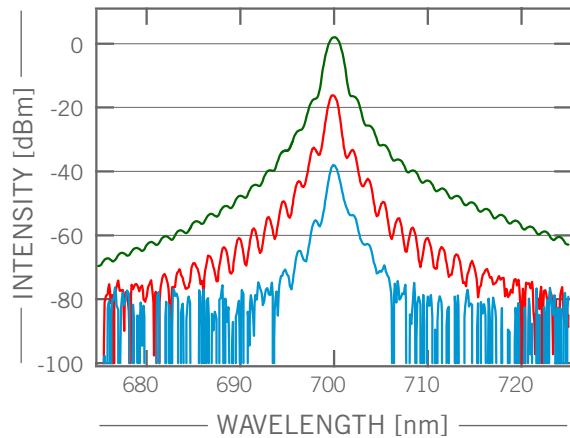


FIG. 4 : LLTF Contrast™ output power spectrum for different SC laser. The noise floor of the measurement is around -80 dBm. **Green** : Fianium’s WL SC480-10 (10 W total output power,  $\approx 8 \text{ mW/nm}$  @700 nm), **red** : Fianium’s WL SC400-4 (4 W total output power,  $\approx 2.1 \text{ mW/nm}$  @700 nm), **blue** : Leukos SM30 (100 mW total output power,  $\approx 0.03 \text{ mW/nm}$  @700 nm).

#### 4.1\_ OUT-OF-BAND MEASUREMENT

To obtain the out-of-band rejection (FIG. 3), a supercontinuum source is first injected in the filter (LLTF™ Contrast) and, once filtered, is recoupled in a fiber (achromatic 10 mm focal lens, multimode 50/62.5  $\mu\text{m}$ ). The signal is then sent to an OSA (ANDO AQ6315E) for detection. FIG. 4 displays the out-of-band rejection obtained with this setup for different supercontinuum sources, but always using the same filter. As mentioned before, the higher the power delivered by the source is, the less likely the measurements will be limited by the noise floor of the detector (around -80 dBm in this case). FIG. 4 illustrates the effect of this limitation; we see that the measured out-of-band rejection using a low power SC only reaches -40 dB<sup>4</sup> (blue curve FIG. 4). It is important to note that this measurement does not reflect the real performance of the filter, but only the limitations of the measuring instrument, hence the importance of using a sufficiently powerful source. When using a medium power SC laser (red curve in FIG. 4), we are able to measure the specified -60 dB out-of-band rejection at  $\pm 25 \text{ nm}$  from the central wavelength. Finally, when using a high power SC laser (green curve in FIG. 4), we can also measure the specified -60 dB out-of-band rejection, but this time at an even closer distance from the central wavelength ( $\pm 21 \text{ nm}$ ).

4. To obtain the out-of-band rejection in dB from dBm measurements, one have to refer to the aforementioned definition of those specifications :  $\text{dB} = 10(\log_{10} P_1 - \log_{10} P_0)$  and  $\text{dBm}_1 = 10(\log_{10} P_1 - \log_{10} 1\text{mW})$ , hence  $\text{dB} = \text{dBm}_1 - \text{dBm}_0$ .

## 4.2\_ OPTICAL DENSITY MEASUREMENT

Measuring the OD ( $\log_{10}(I_0/I_t)$ ) is even more challenging than the out-of-band rejection because for any given wavelength we need to measure the intensities of the supercontinuum source ( $I_0$ ) and the filtered beam ( $I_t$ ) with the exact same conditions. As displayed in FIG. 5, the 1064 nm pump residual of the SC laser is the perfect reference mark to help us measure the real OD. It is the only spectral feature where there is signal outside of the out-of-band rejection span and above the measurement noise limit. In FIG. 5 we see the noise floor at around -76 dBm and the emerging 1064 nm pump residual. To obtain the optical density, we use the experimental configuration described in FIG.3. The measurements are repeated sequentially, once with the light path passing through the VBG, once using the mirrors' path. By comparing the two intensity peaks at 1064 nm (FIG. 5), an OD of 6.8 is found.

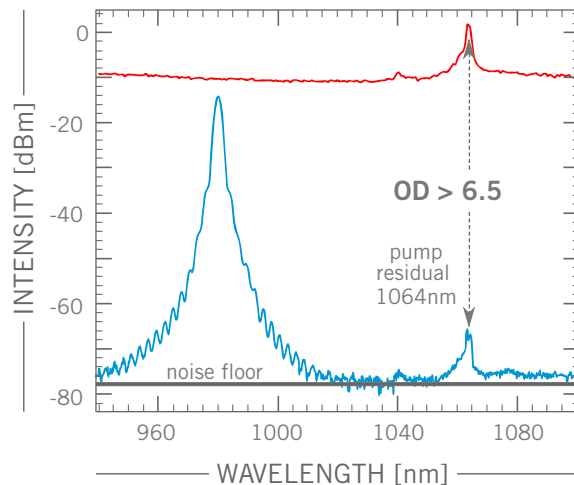


FIG. 5 : Measurements of the optical density ( $OD = \log_{10}(I_0/I_t)$ ) at the pump energy (1064 nm). **Blue**: LLTF Contrast™ output ( $I_t$ ), **Red**: unfiltered supercontinuum output ( $I_0$ ). Those measurements were realised with the setup shown in FIG. 3.

## 5\_ CONCLUSION

Apart from the covered spectral range and bandwidth, two important optical characteristics of a widely tunable filter are the out-of-band rejection and the optical density. It is essential to have in mind the definitions of these characteristics when choosing such a filter. In this white paper, the out-of-band rejection of an optical bandpass filter is defined as the ability to select precise wavelengths, but to attenuate to very low levels those outside a specific band. Also, the OD is defined as the logarithmic ratio between the radiated power of the incident beam and the radiated power transmitted through the instrument.

Manufacturers do not necessarily use the same definitions and confusion may arise when trying to compare specifications from one supplier to another. Do not hesitate to contact them in order to clarify their specifications and meaning. Finally, if you wish to perform the measurements to validate the specifications, be aware that the out-of-band rejection requires a very sensitive and high dynamic range measurement setup. Concerning the OD, the measurement is done in the manufacturing process and cannot be accurately repeated by customers.

## **AUTHORS PROFILE**

Daniel Gagnon is Director of production and mechanical engineering at Photon etc. He is in charge of manufacturing operations, mechanical engineering, and the introduction of new products & processes into production. Daniel also manages the development of the Laser Line Tunable Filter and Widefield Hyperspectral imager product lines. Daniel has over 15 years of experience including R&D, product development (NPD) from concept to mass production, project management, engineering management and optomechanical systems design. He holds a bachelor's degree in mechanical engineering and a master's degree in optomechanics & innovation management.

Laura-Isabelle Dion-Bertrand is an Application Scientist at Photon etc. She is in charge of product development, marketing and sales. She holds a BS in physics and a master's degree in condensed matter physics from Université de Montréal. Her deep understanding of material sciences has led to numerous publications in collaboration with researchers worldwide. Laura's expertise has opened new application territories for Photon etc's hyperspectral imaging systems.

For more information contact Photon etc. Inc. as follows:  
dgagnon@photonetc.com or sales@photonetc.com

## APPENDIX 1

### HOW DOES A VOLUME HOLOGRAPHIC BRAGG FILTER WORK

Photon etc.'s core technology is a continuously tunable filter [3] based on thick holographic gratings, also referred to as Volume Bragg Gratings (VBG) [4,5]. The gratings are made of silver halide glass, a non-hygroscopic material transparent between 400 and 2500 nm. This photo-thermo-refractive (PTR) glass [6,7] has a periodically varying index of refraction in which the modulation structure is oriented to either transmit or reflect incident light. The refractive index variations achievable with this type of glass is however low (i.e.  $\Delta n \approx 10^{-4}$ ) in comparison to other competing materials such as dichromated gelatin. Nevertheless, the greater optical path attainable with VBGs (i.e. thickness of a few mm) overcomes this apparent limitation. Also, saturated Bragg gratings made of PTR glass can reach theoretical efficiencies higher than 99 % [8], with a very narrow bandwidth (down to a few hundreds of picometers), and a weak polarisation sensitivity.

VBGs can be fully described by the following parameters (see FIG. A1) [8]: the thickness of the grating, the refractive index of PTR glass ( $n_0$ ), the period ( $\Lambda$ ) of the grating (or spatial frequency  $f = 1/\Lambda$ ), the angle ( $\Theta$ ) between the incident beam and the normal of the entrance surface ( $\vec{N}$ ), and the inclination of the Bragg planes ( $\phi$ ) defined as the angle between the normal ( $\vec{N}$ ) and the grating vector ( $\vec{K}_g$ ).

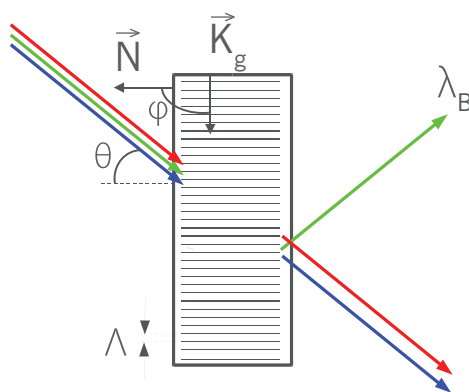


FIG. A1: Schematic of a volume holographic transmission grating.

Like shown in FIG. A1, the incoming collimated light is diffracted by the volume holographic filter, and only a small fraction of the spectrum is affected. In order to select which particular wavelength will be diffracted, the angle of the filter is adjusted to meet Bragg's condition:

$$\lambda_B = 2n_0\Lambda\cos(\Theta+\Phi)$$

where  $\lambda_B$  is the diffracted wavelength. Like shown in FIG. A1, for transmission gratings,  $\phi = \pi/2$  (Bragg planes are perpendicular to the entrance surface). In this case, the Bragg condition becomes:

$$\lambda_B = 2n_0\Lambda\sin\Theta$$



As mentioned, this condition is valid for transmission gratings and has to be altered for reflection gratings where Bragg planes are parallel to the entrance surface. For reflection gratings,  $\phi = 0$  and the Bragg condition becomes:

$$\lambda_B = 2n_0\Lambda\cos\Theta$$

If the beam does not meet the Bragg condition, it passes through the filter undiffracted. To illustrate the behavior of the diffracted fraction of the beam, we present a typical diffraction efficiency spectrum of a transmission Bragg grating (see FIG. A2). This spectrum was plotted using the diffraction efficiency equation obtained with the Kogelnik theory of thick hologram gratings [9]. As can be observed in FIG. A2, the theoretical diffraction efficiency peak of this grating reaches 98 % for a central wavelength of  $\lambda_c = 632$  nm. The FWHM is equal to 1.8 nm, and the first side lobe peaks are located around 11,8 % (-9.3 dB) below the main peak. This theoretical spectrum illustrates the intrinsic ability of VBGs to diffract a narrow band of a given wavelength, and attenuate the rest to extremely low levels.

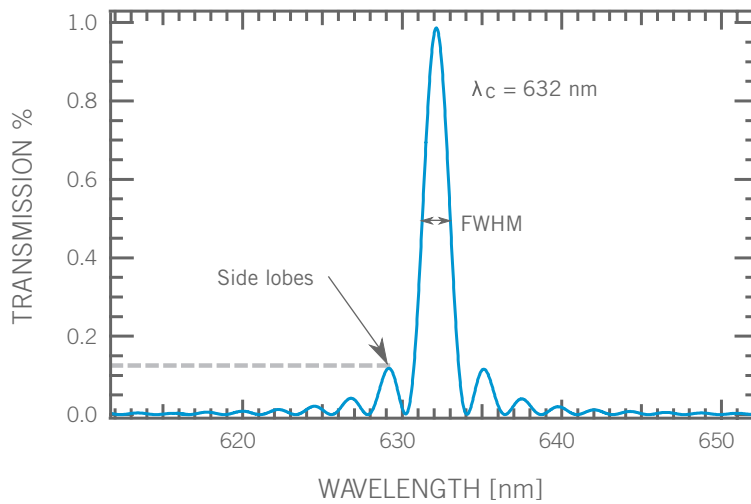


FIG. A2: Illustration of the diffraction efficiency of a volume holographic grating. The theoretical diffraction efficiency peak reaches 98 % at 632 nm. The FWHM is 1.8 nm, and the first side lobe peaks are located at 11,8 % (-9.3 dB).

## APPENDIX 2

### CREATING AN ULTRABROAD TUNABLE LASER SOURCE

Widely tunable filters can be coupled with a supercontinuum laser to provide a versatile tool known as a tunable laser source (TLS). Supercontinuum lasers [10] are typically high-power fiber lasers delivering broadband radiation (~400 nm to ~2500 nm). To achieve such ultra broad radiation, a laser beam is directed towards a highly non-linear medium in which a series of nonlinear processes (e.g.: four-wave mixing, Raman shifting of the solitons) interact constructively to create the supercontinuum emission. When coupled with the right filter, it can deliver a quasi-monochromatic output over the whole supercontinuum spectral range (FIG. A3). Such sources are used in various experiments and fields of research; photoluminescence excitation, reflection/absorption spectroscopy, spectrally resolved light beam induced current (LBIC) [11], steady state pump-probe experiment, hyperspectral imaging [12], incoherent light transport experiment [13] and detector calibration [14,15]. Apart from being a great tool for dedicated experiments, the TLS is also well suited as a general laboratory light source, delivering a narrowband wavelength, tunable over a broad range, all within an easy to use turnkey system.

An example of the output power of a TLS is shown in FIG. A3. This plot comes from measurements performed using a Fianium WhiteLase SC-400-4 source, the VIS and SWIR versions of the LLTF Contrast™ to cover the whole range of the SC laser, and a Gentec pyroelectric detector (Model XPL 12) to measure the output power.

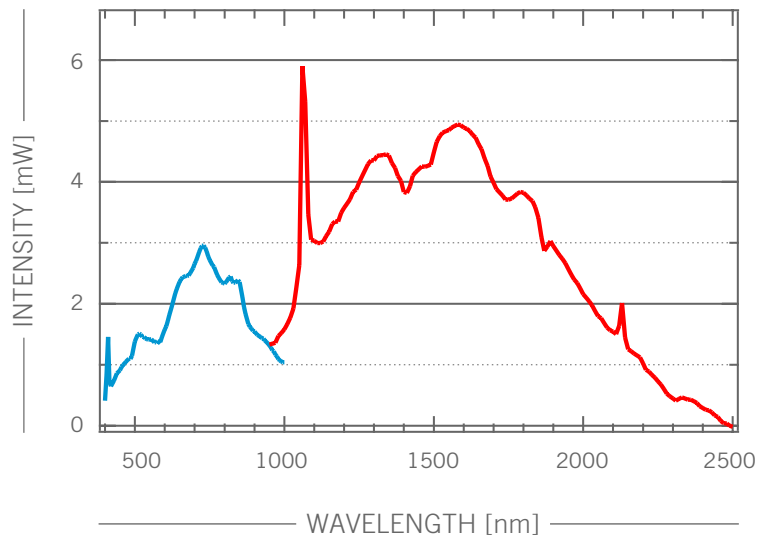


FIG. A3: Output from Photon etc's tunable laser source. Visible option covering 400 - 1000 nm and SWIR option covering 1000 - 2500 nm.

## REFERENCES

- [1] Verhaegen M., Tunable laser source exhibits out-of-band rejection of  $10^{-6}$  [Online], Laser Focus World, **2010**, 46(3), (accessed April 8, **2015**).
- [2] Nic M., Jirat J. , Kosata B., updates compiled by Jenkins A., IUPAC Gold Book [Online], Blackwell Scientific Publications, 2nd edition, **2006** - , (accessed April 8, **2015**).
- [3] S. Blais-Ouellette; Method and apparatus for a Bragg grating tunable filter, U.S. Patent 7557990 (B2), July 7, **2009**.
- [4] Efimov O.M., Glebov L.B., Glebova L.N., Richardson K.C., and Smirnov V.I., High efficiency Bragg gratings in photo-thermo-refractive glass, Appl. Opt., **1999**, 38(2).
- [5] Glebov A. L., Mokhun O., Rapaport A., Vergnole S., Smirnov V.I., Glebov L. B., Volume Bragg Gratings as Ultra-Narrow and Multiband Optical Filters, Invited Paper, Proc. of SPIE, **2012**, 8428.
- [6] Kuchinskii S.A., Nikonorov N.V., Panysheva E.I., Savvin V.V., and Tunimanova I.V., Properties of volume phase holograms on polychromatic glasses, Optics and Spectroscopy, **1991**, 70(6).
- [7] Glebov L.B., Nikonorov N.V., Panysheva E.I., Petrovskii G.T., Savvin V.V., Tunimanova I.V., and Tsekhomskii V.A., New possibilities of photosensitive glasses for the recording of volume phase holograms, Optics and Spectroscopy, **1992**, 73(2).
- [8] Ciapurin I. V., Glebov L. B., and Smirnov V.I., Modeling of Gaussian beam diffraction on volume Bragg gratings in PTR glass, Proc. of SPIE, Practical Holography XIX: Materials and Application, **2005**, 5742.
- [9] Kogelnik H., Coupled wave theory for thick hologram gratings, The Bell System Technical Journal, **1969**, 48(9).
- [10] Devine A., and Grudinin A., Supercontinuum sources : An even brighter future awaits supercontinuum fiber lasers [Online], Laser Focus World, **2013** (accessed April 22, **2015**).
- [11] Lombez L. , Ory D., Paire M., Delamarre A., Hajje G.E., Guillemoles J.F., Micrometric investigation of external quantum efficiency in microcrystalline  $\text{CuInGa}(\text{S,Se})_2$  solar cells, Thin Solid Films, **2014**, 565.
- [12] Shahidi A.M., Patel S.R., Flanagan J.G. and Hudson C., Regional variation in human retinal vessel oxygen saturation, Experimental Eye Research, **2013**, 113.
- [13] Chaudemanche S., Ponçot M., André S., Dahouna A., and Boursonb P., Evolution of the Raman backscattered intensity used to analyze the micromechanisms of deformation of various polypropylene blends in situ during a uniaxial tensile test, J. Raman Spectrosc. **2014**, 45(5).
- [14] Sivaramakrishnan A., Soummer R., Oppenheimer B.R., Roberts R., Brenner D., Carlotti A., Pueyo L., Macintosh B., Bauman B., Saddlemyer L, Palmer D., Erickson D., Dorrer C., Caputa K., Marois C., Wallace K., Griffiths E. and Mey J., The Gemini Planet Imager coronagraph testbed, Proc. SPIE 7440, Techniques and Instrumentation for Detection of Exoplanets IV, **2009**, 74400.

[15] A.P. Levick, C.L. Greenwell, J. Ireland, E.R. Woolliams, T.M. Goodman, A. Bialek, et al. Spectral radiance source based on supercontinuum laser and wavelength tunable bandpass filter: The spectrally tunable absolute irradiance and radiance source, *Applied Optics*, **2014**, 53.